Journal of Applied Biological Sciences 7 (3): 90-98, 2013
ISSN: 1307-1130, E-ISSN: 2146-0108, www.nobel.gen.tr

Numerical and Experimental Analyses of a Sandy Soil Water Movement under a Point Source Using Dynamic Pore Network Modeling

Saeed SAMADIANFARD* Ali Ashraf SADRADDINI Amir Hosein NAZEMI

Water Engineering Department, Faculty of Agriculture, University of Tabriz, Tabriz, Iran

*Corresponding author:
E-mail: s.samadian@tabrizu.ac.ir

Received: November 30, 2013
Accepted: December 31, 2013

Abstract

Water flow simulation in porous medium such as soil is an important topic in several branches of hydrology, soil science and agricultural engineering. In the present study, numerical results from a dynamic pore network model were used to determine a macroscopic relationship between capillary pressure and fluid saturations. Then using the resulted relationship from pore network modeling and solving the partial differential Richards' equation by finite difference scheme (PNMCRE), water movement in the soil has been simulated. Also, soil water movement was investigated by laboratory experiments on sandy soil. The performance of PNMCRE was evaluated by comparing the simulated wetting fronts with both of the observed patterns and those simulated by HUDRUS software package. Statistical analysis showed that PNMCRE model with minimum errors and high correlation coefficients for all discharge rates and in time intervals had a better agreement with observed patterns in comparison with HYDRUS 2D.

Keywords: dynamic pore network, HYDRUS 2D model, laboratory experiments, Richards' equation

INTRODUCTION

Information on moisture distribution patterns in porous media is necessary for the proper design and operation of complex systems in different branches of applied sciences such as hydrology, agricultural and petroleum engineering. The moisture distribution pattern is influenced by the soil properties and the manner water is applied and withdrawn from the soil profile. Flow from a point-source, because of its multi-dimensional nature, leads to complexities in modeling of the soil moisture dynamics.

Mathematical models have been proven very useful for predicting water movement through the soil [1], but they need a primer knowledge about laboratory water retention parameters which is somehow difficult to be obtained. Philip [2] developed a mathematical theory for a two- and three-dimensional unsaturated water flow from buried point sources and spherical cavities. Schwartzman and Zur [3] studied the geometry of the wetted soil volume under point source and developed a series of empirical equations relating the width and depth of the wetted soil volume to the discharge of point source, saturated hydraulic conductivity of the soil and volume of the water in the wetted soil volume. Clark et al. [4] reported that the lateral movement of water varied in the range of 15.5 - 20 cm for discharge rates of 1.5 - 1.9 $L.hr^{-1}$ from a point source in a sandy soil. Or [5] investigated the effects of mild spatial variation of soil hydraulic properties on wetting pattern of different soils. Smith and Warrick [6] presented basic relations of soil water flow to measure the soil water content, pressure head and hydraulic conductivity. They also discussed on calculation procedures of soil infiltration rates and the measurement of soil infiltration parameters, as well as on many of the complexities and challenges for applying the current understanding of water movement in the soil.

Numerical methods also have been developed to simulate this phenomenon [7,8,9]. For instance, HYDRUS 2D is a model based on finite-element numerical solutions of the flow equations [10], allowing simulations of three-dimensional axially symmetric water flow. Many studies proved the capabilities of HYDRUS 2D model for simulation of water and solute transport in different soils [11, 12, 13, 14, 15, 16].

Pore-scale modeling has been widely used as a platform to study multiphase flow in petroleum engineering, hydrology and environment engineering [17, 18, 19] and offers an alternative to empirical models. Pore-scale or network models can be used to predict multiphase flow behavior by simulating the flow process based on a detailed description of the pore structure, fluid characteristics, and the governing pore-scale displacement mechanisms. The pore space in a porous medium is represented by a network of pores (corresponding to the larger void spaces) and throats (the narrow openings connecting the pores) with parameterized geometries and topology through which multiphase flow can be simulated.

Network models were first developed by Fatt [20] based on the idea that pore space might be represented as an interconnected network of capillary tubes whose radii would represent the dimensions of the pores within a porous medium. Koplik and Lasseter [21] simulated primary drainage in networks of spherical pores connected to cylindrical pore throats. Touboul et al. [22] and Blunt et al.

[23] used a simplification of the model of Koplik, assuming that the pores had volume but no resistance to flow and the throats had resistance to flow but no volume. Valvanides and Payatakes [24] simulated water flow in a network of spherical chambers connected through long cylindrical throats with a sinusoidally varying cross section. Dahle and Celia [25] extended the model of Blunt et al. [23] to study the effect of material heterogeneities on the capillary pressure-saturation relationship, effect of nonzero stress at the fluid-fluid interface, interfacial area and its relation to capillary pressure, and interfacial velocity. Singh and Mohanty [26] developed a dynamic model to simulate two-phase flow. They used a cubic network with cubic pores and throats of square cross section. The model was used to study primary drainage with constant inlet flow rate. Saturation and relative permeability were computed as a function of capillary number, viscosity ratio, and pore-throat size distribution. Fenwick and Blunt [27] investigated wedge and corner flows with an angular representation of pore throats within a network model. Reeves and Celia [28] employed a three-dimensional network of interconnected pores and throats to simulate drainage and imbibition processes in a strongly water-wet air–water system. Their results showed a smooth functional relationship between capillary pressure, saturation and interfacial area in a wide range of capillary pressure and saturation. Held and Celia [29] used network modeling to compute relationships between capillary pressure, saturation and interfacial areas. Joekar-Niasar et al. [30] used a tube network model, in which zero volume was assigned to the nodes, as well as a sphere-and-tube model to study the water – air interfacial area relationships with capillary pressure and saturation in two-phase systems through primary drainage and imbibition simulations. The authors included phase entrapment caused by piston-like mechanism in their work.

Although mathematical and numerical models have been proven very appropriate in simulation of water flow in porous media, but in these models, the prior knowledge of water retention parameters is mandatory for further simulations. The mentioned parameters usually can be obtained in two ways: 1) By performing laboratory experiments with pressure plate membrane which are time consuming. 2) By using software packages like Rosetta or RETC which implement a number of pedotransfer functions to predict water retention parameters of soil hydraulic models such as Van Genuchten [31] from readily accessible soil data and therefore these predictions are not reliable. The goal of this study is to propose an alternative way based on dynamic pore network modeling and solving partial differential Richards' equation by finite difference scheme for simulation of water movement in the sandy soil under a surface point source. This mentioned approach uses only grain size distribution curve for computation of water retention parameters. The accuracy of the proposed method has been verified by comparison with the observation as well as HUDRUS 2D results.

MATERIALS AND METHODS

Dynamic pore network model

In this research we have used a dynamic pore network model proposed by Joekar-Niasar et al. [32]. The mentioned pore network model has a three-dimensional regular lattice structure with fixed coordination number of six. Pore bodies have cubic shape and pore throats have square cross sections. Fig. 1 shows a schematic presentation of two pore bodies and the connected pore throat. Additional details about dynamic pore network model can be found in Joekar-Niasar et al. [32].

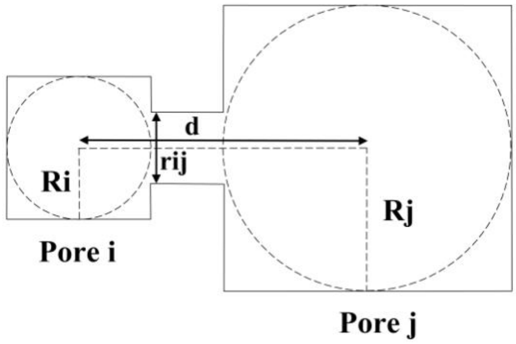

Fig. 1 Schematic presentation of two pore bodies and the connected pore throats

Numerical solving of Richards' equation using finite difference scheme

The Richards' equation (Richards [33]) is the most general method to compute soil moistures and hydrological fluxes, such as infiltration in porous media. Consider two- and/or three-dimensional isothermal uniform Darcian flow of water in a variably saturated rigid porous medium and assume that the air phase plays an insignificant role in the liquid flow process. The governing flow equation for these conditions is given by the following modified form of the Richards' equation (Bear [34]):

$$C\frac{\partial h}{\partial t} = \frac{1}{r}\frac{\partial}{\partial r}\left(rK(h)\frac{\partial h}{\partial r}\right) + \frac{\partial}{\partial z}\left(K(h)\frac{\partial h}{\partial z}\right) - \frac{\partial K}{\partial z} - S(r,z,t,h)$$
(1)

where C= specific capacity of water (m^{-1}), h= pressure head (m), r, z= radial and vertical directions, t= time (hr), S= sink term (hr^{-1}) and K= unsaturated hydraulic conductivity function ($L.hr^{-1}$).

The general form of Richards' equation after discretization, linearization and simplification can be expressed as (Besharat et al. [35]):

$$C_{i,j}^{n}\frac{h_{i,j}^{n+1/2}-h_{i,j}^{n}}{\Delta z_i} = \frac{K_{i+1/2,j}^{n+1/2}\left(h_{i+1,j}^{n+1/2}-h_{i,j}^{n+1/2}\right)-K_{i-1/2,j}^{n+1/2}\left(h_{i,j}^{n+1/2}-h_{i-1,j}^{n+1/2}\right)}{(\Delta r)^2}$$
$$+\frac{K_{i,j}^{n+1/2}}{i\Delta\Delta}\frac{\left(h_{i+1,j}^{n+1/2}-h_{i-1,j}^{n+1/2}\right)}{2\Delta\Delta}+\frac{K_{i,j+1/2}^{n}\left(h_{i,j+1}^{n}-h_{i,j}^{n}\right)-K_{i,j-1/2}^{n}\left(h_{i,j}^{n}-h_{i,j-1}^{n}\right)}{(\Delta z)^2}$$
$$-\frac{\left(K_{i,j+1}^{n}-K_{i,j-1}^{n}\right)}{2\Delta\Delta}-S_{i,j}^{n}$$
(2)

In Eq. 2, superscript n refers to the current time step and superscript n+1/2 denotes the arithmetic mean of a parameter at time steps n and n+1. Furthermore, unsaturated hydraulic conductivity function (K) is defined by:

$$K = K_s S_e^{\,l}\left[1-\left(1-S_e^{1/m}\right)^m\right]^2$$
(3)

where K_s= saturated hydraulic conductivity ($m.hr^{-1}$), Se= effective saturation (-), m and l= shape parameters (-). For K, we take the geometrical mean as proposed by Vauclin et al. [36].

$$K_{i+1/2,j} = \sqrt{K_{i+1,j} \times K_{i,j}}$$
(4)
$$K_{i-1/2,j} = \sqrt{K_{i-1,j} \times K_{i,j}}$$
(5)

It should be noted that a third-type (Cauchy type) boundary condition is used to prescribe the water flux from point source in the soil surface and constant water content has been used as initial condition in numerical scheme [37].

Numerical simulation of water movement under a surface point source using HYDRUS 2D

HYDRUS 2D which uses the Galerkin finite-element method to solve partial differential Richards' equation was applied to simulate the three dimensional axial symmetric water flow. Simulations were carried out considering a 100 cm deep and 120 cm wide soil profile, where a point source was placed on the soil surface. The computational flow domain was made large enough to ensure that the side and bottom boundaries did not affect the simulations. Absence of flux was considered along the surface and the lateral boundaries and free drainage along the bottom boundary of the soil profile. A constant flux density corresponding to the point source discharge rate was assumed along the surface boundary. Also initial water content in whole domain was assumed as initial condition. An unstructured mesh was automatically generated to discretize the flow domain into triangles. A total of 4658 nodes were used to represent the entire simulation domain. Furthermore, the trial and error procedure has been used for selecting the best mesh size. Fig. 2 shows the scheme of the grid used for the numerical simulations by HYDRUS 2D.

Laboratory experiments

For evaluating the accuracy of the proposed PNMCRE and HYDRUS 2D models, experiments of water infiltration under point source were conducted on a sandy soil (90% sand, 5% silt and 5% clay). Laboratory experiments were carried out using a 120 cm × 120 cm × 120 cm transparent Plexiglas box (as shown in Fig. 3). Air dried sand with a mean particle size d_{50} = 0.4 mm was compacted at predetermined dry bulk density of 1.5 $g.cm^{-3}$. A polyethylene pipeline connected to water reservoir was laid on the soil surface which had a 16 mm outside diameter, a wall thickness of 2 mm and used for supplying the discharge rate of 2, 4 and 6 $L.hr^{-1}$. During operation, wetting pattern dimensions were measured using high performance photography and were analyzed by Digimizer Software. The observed soil wetting pattern had a high degree of horizontal symmetry.

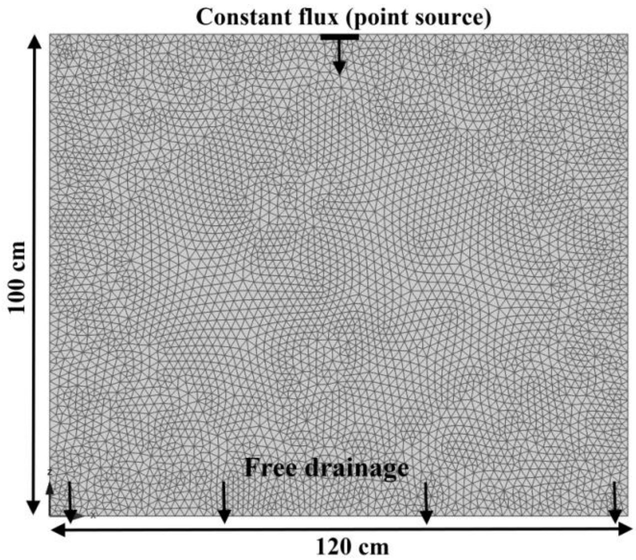

Fig. 2 Scheme of the finite element grid used in the numerical simulations

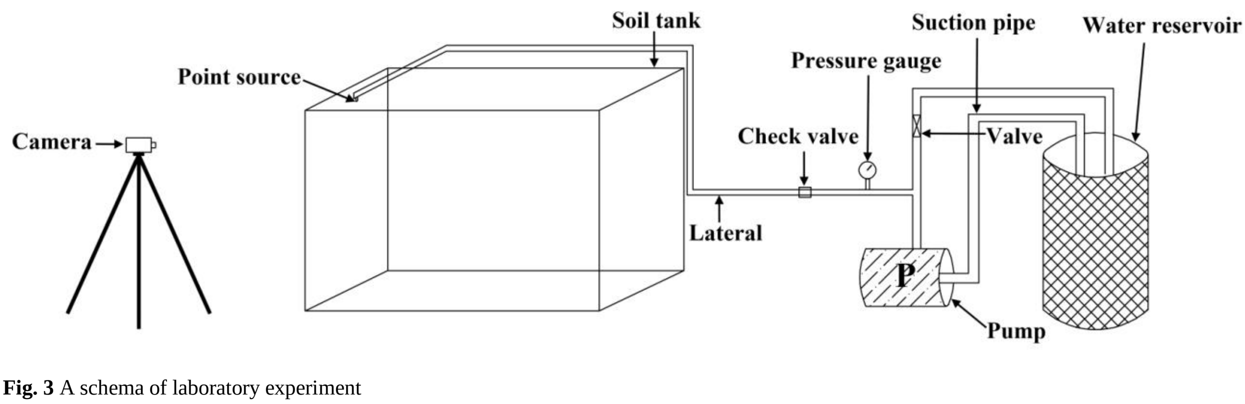

Fig. 3 A schema of laboratory experiment

Evaluation parameters

Several parameters can be considered for the evaluation of radius and depth of wetting pattern estimates. In this study the following statistic criteria were used: correlation coefficient (R), mean absolute error (MAE), root mean squared error (RMSE) and index of agreement (IA).

$$R = \frac{\left(\sum_{i=1}^{n} x_i y_i - \frac{1}{n}\sum_{i=1}^{n} x_i \sum_{i=1}^{n} y_i\right)}{\sqrt{\left(\sum_{i=1}^{n} x_i^2 - \frac{1}{n}\left(\sum_{i=1}^{n} x_i\right)^2\right)\left(\sum_{i=1}^{n} y_i^2 - \frac{1}{n}\left(\sum_{i=1}^{n} y_i\right)^2\right)}} \quad (6)$$

$$MAE = \frac{1}{n}\sum_{i=1}^{n}\left|x_i - y_i\right| \quad (7)$$

$$RMSE = \sqrt{\frac{1}{n}\sum_{i=1}^{n}(x_i - y_i)^2} \quad (8)$$

$$IA = 1 - \frac{\sum_{i=1}^{n}(x_i - y_i)^2}{\sum_{i=1}^{n}\left(\left|x_i - \bar{y}\right| + \left|y_i - \bar{y}\right|\right)^2} \quad (9)$$

where x_i = distance from point source computed by PNMCRE and HYDRUS 2D (cm), y_i = observed distance from point source (cm) and n = number of values.

RESULTS AND DISCUSSION

As were mentioned earlier, the studied pore network model had a three dimensional regular lattice structure. In this network, each pore body was connected with six pore throat. Also it was assumed that the volume of pore throats was negligible compared to the volume of pore bodies. Fig. 4 shows a sample of the developed pore network with 10 pore bodies in each direction. It should be noted that all computations related to dynamic pore network modeling and numerical solving of partial differential Richards' equation by finite difference scheme were done by an algorithm which has been developed in Wolfram Mathematica 8.0.

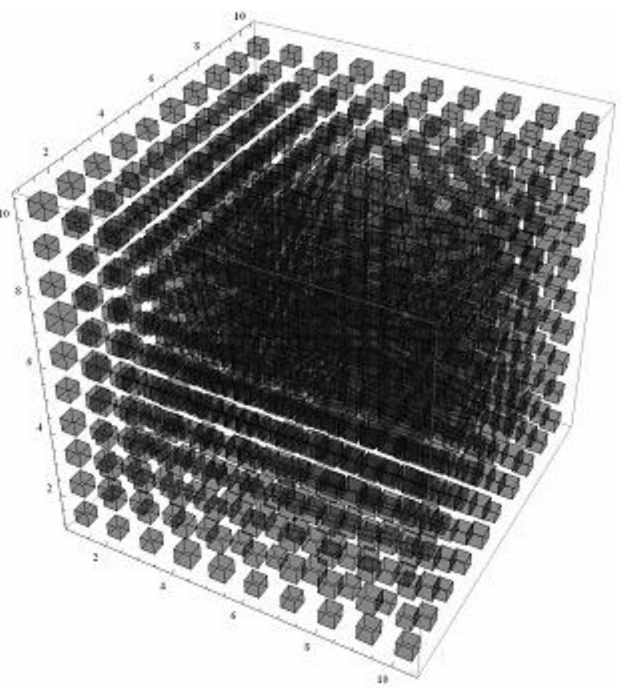

Fig. 4 A sample of developed pore network with 10 pore bodies in each direction

To achieve an optimum pore network size, series of computations were done using the developed algorithm in Wolfram Mathematica 8.0. For this purpose, 6 different networks by having 12, 16, 20, 24, 28 and 32 pore bodies in each direction have been considered. These simulations took 4 to 170 hours on Intel (R) Core(TM) i3 CPU, 3.07 GHz with 4 GB RAM, which is somehow time consuming process. The resulted capillary pressure – saturation relationships for different networks are shown in Fig. 5.

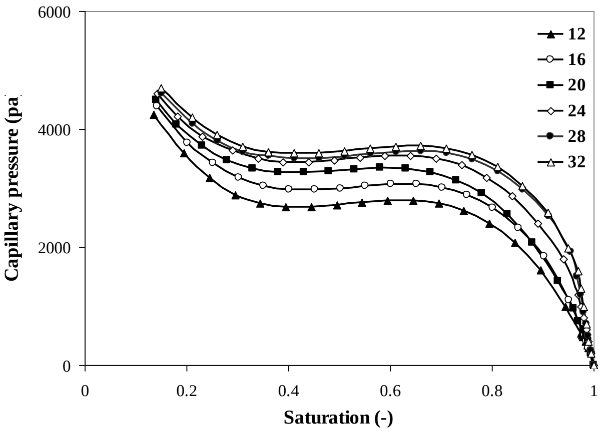

Fig. 5 Resulted capillary pressure – saturation relationship for different networks

It is obvious from Fig. 5 that capillary pressure - saturation curve changes with the network size until a network size of 28×28×28 pore bodies and then this change in mentioned curves is negligible at networks with more than 28 pore bodies in each direction. Therefore, resulted curve from selected network with 32 pore bodies in each direction was used for simulating wetting front in macro scale. Table 1 shows the network specifications used in the simulations.

Table 1. Pore network parameters

Specification	Value	Unit
Lattice dimension	32 × 32 ×32	-
Lattice size	29 × 29 ×29	mm^3
Min. pore body inscribed radius	0.320	mm
Max. pore body inscribed radius	0.496	mm
Mean pore body inscribed radius	0.405	mm
Standard deviation	0.024	mm

After selecting the representative network with 32 pore bodies in each direction, simulations of water movement in the sandy soil was continued by using the resulted capillary pressure – saturation relationship from dynamic pore network simulations. Then whole domain with 100 cm depth and 120 cm width was divided to a grid with 1 cm intervals and an algorithm has been developed in Wolfram Mathematica 8.0. Also, wetting pattern under the point source were simulated by solving Richards' equation with finite difference scheme (PNMCRE). The results of PNMCRE and HYDRUS 2D simulations for different discharge rates (Q) and time durations (D) are presented in Fig. 6.

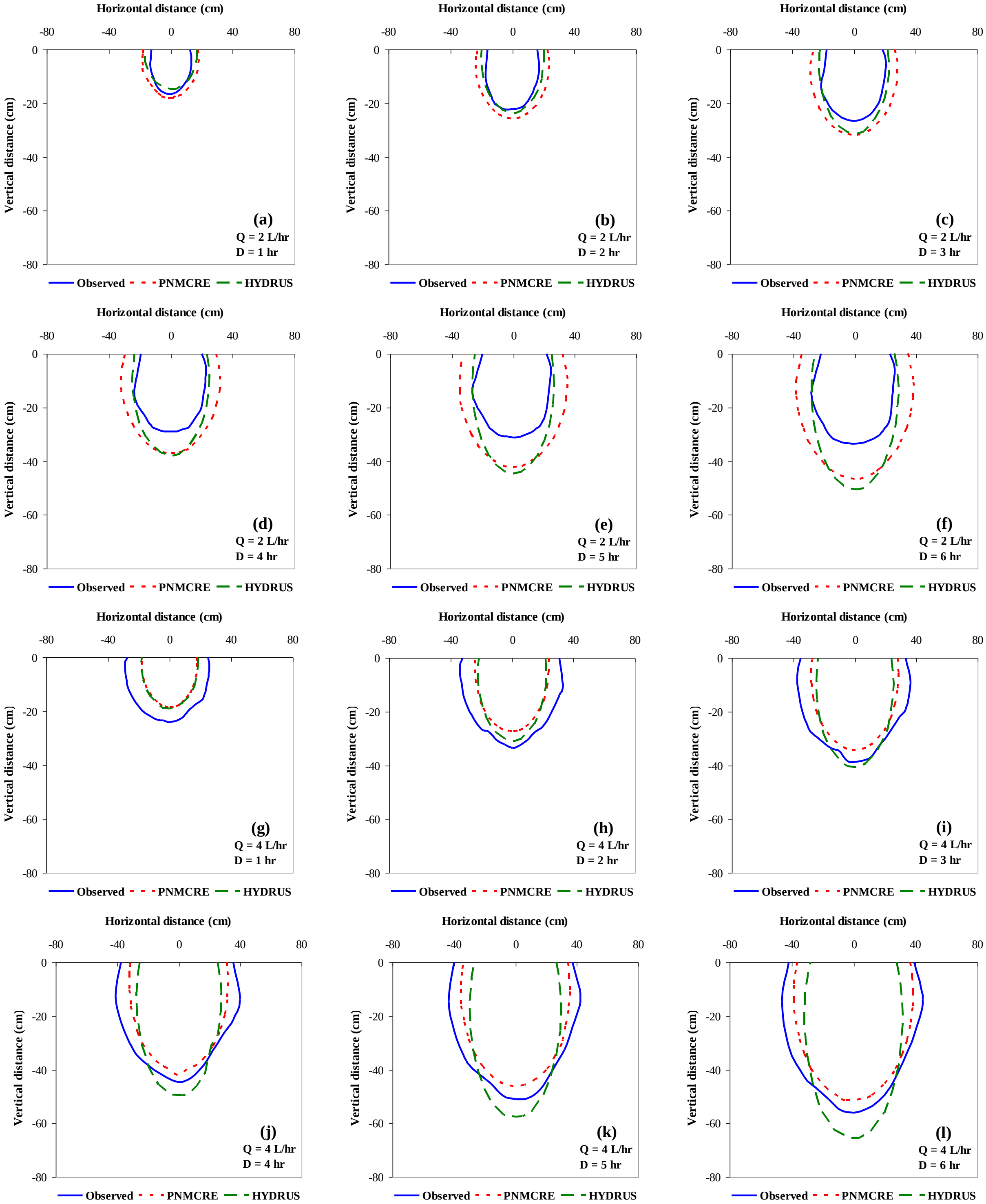

Fig. 6 Illustration of the observed and simulated wetting fronts in sandy soil under the point source with discharge rates of 2, 4 and 6 $L.hr^{-1}$ and duration of 1 to 6 h. (Q: discharge rate and D: time durations)

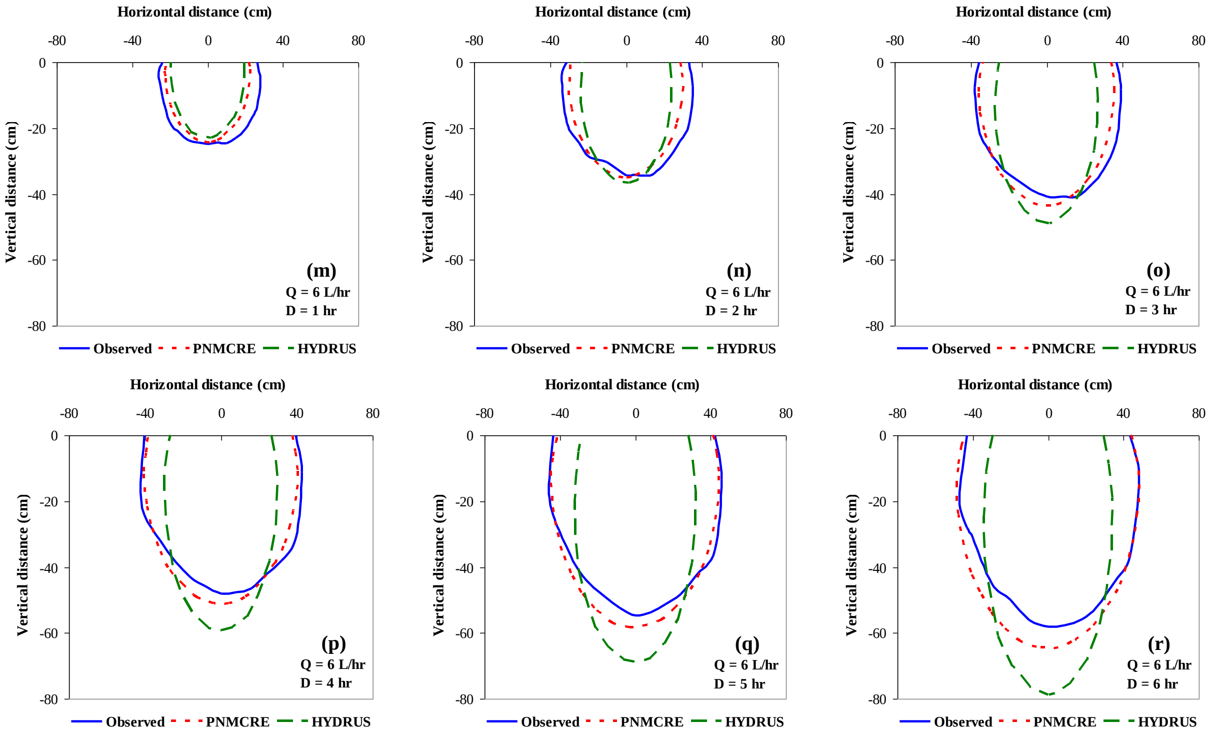

Fig. 6 Continued

The illustrated patterns in Fig. 6 are for the time duration of 1, 2, 3, 4, 5 and 6 h from the beginning of experiments and for three discharge rates of 2, 4 and 6 L.hr^{-1}. The HYDRUS 2D model output data are closer to the observed wetting fronts than those of the PNMCRE model with discharge rates of 2 L.hr^{-1} in all durations (Fig. 6). The estimated wetting fronts via implementation of PNMCRE in low discharge rates have not very good agreement with the observed data. PNMCRE model gives better estimates than HYDRUS 2D with the discharge rates of 4 and 6 L.hr^{-1}. As it is clearly seen from Fig. 6, the HYDRUS 2D simulated wetting fronts are more stretched than those observed and simulated with PNMCRE in the cases of supplying 4 and 6 L.hr^{-1}. It can be concluded that the PNMCRE model accurately predicts the observed wetting pattern in discharge rates more than 2 L.hr^{-1}. Furthermore, PNMCRE overestimates the radial distances in low discharge rate (2 L.hr^{-1}) and underestimates them in medium discharge rate (4 L.hr^{-1}). But in the case of high discharge rate (6 L.hr^{-1}) it has better predictions in comparison with the two aforementioned discharge rates in all directions. On the other hand, this trend is not seen in the predictions of the HYDRUS 2D model. Overally, it can be concluded that PNMCRE estimations are closer to the corresponding observed values than those of the HYDRUS 2D model. These results suggest that in the case of low discharge rates, PNMCRE may not give any significant advantage over the HYDRUS 2D model. For evaluating accuracy of the proposed PNMCRE and HYDRUS 2D model, the radial distances of wetting pattern from point source with direction angle of θ (which is shown in Fig. 7) are computed according to the predicted results by each one and using statistical parameters (Eqs. 6-9), accuracies of the both models have been computed as shown in Table 2.

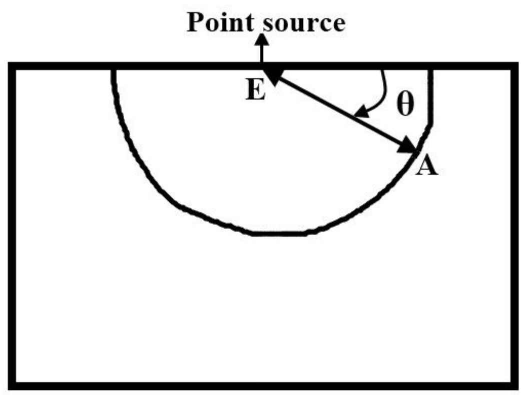

Fig. 7 Illustration of a radial distance (EA) with θ angle from a point source

Table 2 Statistical comparison of PNMCRE and HYDRUS 2D models with observed wetting front distances in different directions from point source

Angle	Model	Statistical parameters				Angle	Model	Statistical parameters			
		R	MAE	RMSE	IA			R	MAE	RMSE	IA
0	PNMCRE	0.752	5.427	6.125	0.855	100	PNMCRE	0.905	4.568	5.273	0.945
	HUDRUS	0.770	8.389	9.349	0.630		HUDRUS	0.959	11.490	13.833	0.804
10	PNMCRE	0.753	6.133	6.706	0.855	110	PNMCRE	0.907	4.511	5.210	0.942
	HUDRUS	0.623	9.513	10.830	0.571		HUDRUS	0.962	9.388	11.339	0.835
20	PNMCRE	0.738	6.741	7.473	0.848	120	PNMCRE	0.893	4.501	5.179	0.940
	HUDRUS	0.818	9.023	10.249	0.688		HUDRUS	0.954	5.352	6.504	0.924
30	PNMCRE	0.779	6.289	7.004	0.877	130	PNMCRE	0.853	5.100	5.758	0.922
	HUDRUS	0.845	7.745	8.518	0.779		HUDRUS	0.928	3.260	4.010	0.962
40	PNMCRE	0.851	5.399	5.999	0.919	140	PNMCRE	0.822	5.428	6.179	0.904
	HUDRUS	0.893	5.747	6.303	0.893		HUDRUS	0.912	4.972	5.447	0.913
50	PNMCRE	0.902	4.154	4.796	0.949	150	PNMCRE	0.798	5.989	6.652	0.885
	HUDRUS	0.939	3.129	3.804	0.967		HUDRUS	0.897	7.107	8.356	0.791
60	PNMCRE	0.917	3.864	4.561	0.957	160	PNMCRE	0.721	6.888	7.806	0.835
	HUDRUS	0.954	4.580	5.639	0.945		HUDRUS	0.823	9.018	10.273	0.688
70	PNMCRE	0.911	4.106	4.861	0.953	170	PNMCRE	0.677	6.998	7.894	0.809
	HUDRUS	0.957	8.137	9.800	0.880		HUDRUS	0.753	9.634	10.670	0.639
80	PNMCRE	0.905	4.322	5.159	0.949	180	PNMCRE	0.702	6.093	7.107	0.818
	HUDRUS	0.957	11.070	13.293	0.821		HUDRUS	0.727	9.079	9.985	0.614
90	PNMCRE	0.901	4.434	5.329	0.946						
	HUDRUS	0.953	11.822	14.180	0.805						

As it can be seen from Table 2, PNMCRE has a better performance than HYDRUS 2D in all directions except at the angles of 50, 130 and 140 degrees. In the mentioned directions, HYDRUS 2D estimates wetting pattern slightly better than PNMCRE. Also IA values of PNMCRE in all directions are higher than the corresponding HYDRUS 2D values except at the angles of 50, 130 and 140 degrees. Finally, for a better comparison of the two mentioned models, their precisions in simulation of the wetting pattern at different discharge rates are evaluated. In this case, the predicted radial distances of wetting front from point source in all directions related to each discharge rate, namely 2, 4 and 6 $L.hr^{-1}$ are presented separately in Figs. 8 and 9. These figures show the scatter plots of observed versus predicted values by PNMCRE and HYDRUS 2D models respectively. Nevertheless, Table 3 shows corresponding statistical comparison of the mentioned models related to Figs. 8 and 9.

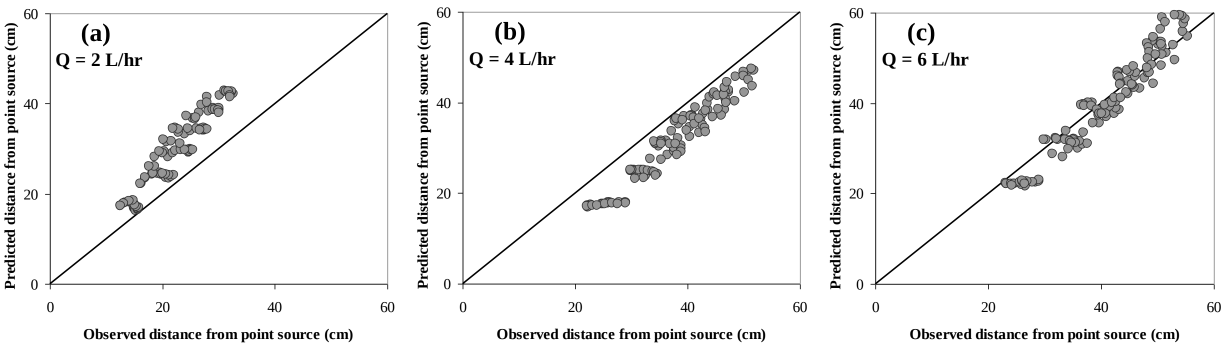

Fig. 8 Scatter plots of the observed (x-axis) and predicted (y-axis) values by PNMCRE for radial distance of point source from wetting front in all directions

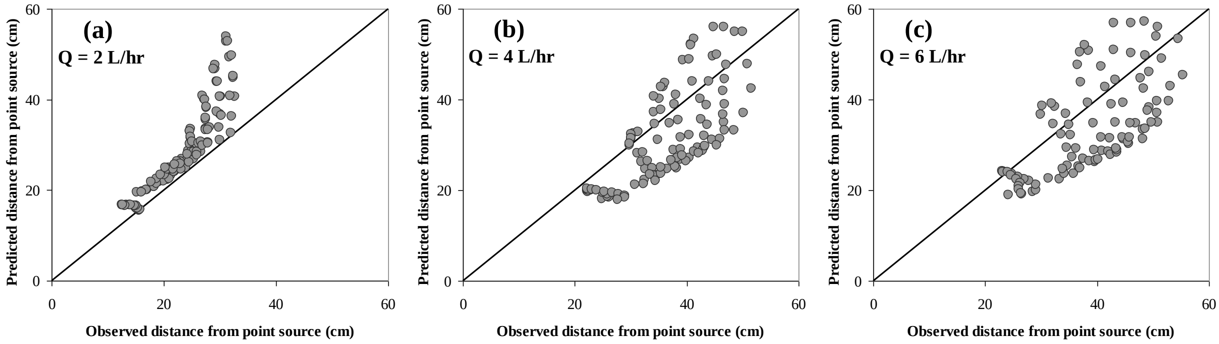

Fig. 9 Scatter plots of the observed (x-axis) and predicted (y-axis) values by HYDRUS 2D for radial distance of point source from wetting front in all directions

Table 3 Performance assessments of PNMCRE and HYDRUS 2D methods for predicting wetting fronts in different discharge rats

Discharge rate ($L.hr^{-1}$)	Model	Statistical parameters			
		R	MAE	RMSE	IA
2	PNMCRE	0.950	7.039	7.767	0.751
	HUDRUS	0.912	5.494	7.464	0.780
4	PNMCRE	0.969	6.023	6.445	0.873
	HUDRUS	0.756	8.079	9.276	0.799
6	PNMCRE	0.968	2.876	3.367	0.972
	HUDRUS	0.698	9.799	11.476	0.765

Significant overestimations and underestimations are seen for the PNMCRE model for the discharge rates of 2 and 4 $L.hr^{-1}$, respectively. Similarly, overestimates can be seen for the HYDRUS 2D model for the discharge rate of 2 $L.hr^{-1}$. Both PNMCRE and HYDRUS 2D models significantly overestimate low discharge rates and underestimate high discharge rates. As can be clearly seen from Fig. 9, too much scattered estimates were obtained from the HYDRUS 2D model in the case of 4 and 6 $L.hr^{-1}$.

CONCLUSION

In this study, dynamic pore network modeling conjuncted by Richards' equation (PNMCRE) was used to simulate wetting patterns under a surface point source. The accuracy of this model was verified by comparison with the more commonly used HYDRUS 2D software and observed data. In the PNMCRE model, based on the grain size distribution curve, the network of pore bodies and throats was constructed and then by dynamic simulation of wetting and nonwetting phases in the mentioned network, water retention curve was computed and used for further simulations of water movement in a sandy soil. The results are promising and allow the users to estimate wetting front dimensions for any given time, discharge rate in the sandy soil without a need to perform detailed laboratory experiments to obtain soil hydraulic properties. Results showed that the PNMCRE model performed better than the HYDRUS 2D model for discharge rates of 4 and 6 $L.hr^{-1}$. Meanwhile, the performance of the HYDRUS 2D model was better than the PNMCRE for discharge rate of 2 $L.hr^{-1}$. The comparison of the results with laboratory experiments revealed that the dynamic pore network models could be employed successfully in modeling water movement in the soil.

Acknowledgment

The financial support from research affairs department of University of Tabriz is gratefully acknowledged.

REFERENCES

[1] Mmolawa K, Or D. 2000. Water and solute dynamics under a drip irrigated crop: experiments and analytical model. *Transaction of the ASAE*. 43, 1597-1608.

[2] Philip JR. 1968. Steady infiltration from buried point sources and spherical cavities. *Water Resource Research.* 4 (5), 1039–1047.

[3] Schwartzman M, Zur B. 1986. Emitter spacing and geometry of wetted soil volume. *Journal of Irrigation and Drainage Engineering -ASCE.* 112, 242-253.

[4] Clark CA, Sranley FS, Zazueta FS. 1993. Qualitative sensing of water movement from a point-source emitter on a sandy soil. *Transaction of the ASAE.* 9 (3), 299-303.

[5] Or D. 1995. Stochastic analysis of soil water monitoring for drip irrigation management in heterogeneous soils. *Soil Science Society of American Journal.* 59, 1222-1233.

[6] Smith RE, Warrick AW. 2007. Soil water relationships- design and operation of farm irrigation systems. *American Society of Agricultural and Biological Engineers (ASABE)*, Ann Arbor (USA). 120-159.

[7] Brandt A, Breslker E, Diner N, Ben-Asher J, Heller J, Goldberg D. 1971. Infiltration from a trickle source: I. Mathematical models. *Soil Science Society of American Journal.* 35, 683-689.

[8] Healy RW. 1987. Simulation of trickle-irrigation, an extension to U.S. Geological Survey's computer program Vs 2D. *US Geological Survey Water Resour Invest 87-4086*, US Govt Washington, DC.

[9] Taghavi SA, Marino Miguel A, Rolston DE. 1984. Infiltration from trickle-irrigation source. *Journal of Irrigation and Drainage Engineering -ASCE.* 0, 331-341.

[10] Simunek J, Van Genuchten MTh, Senja M. 2006. The HYDRUS software package for simulating two-and three-dimensional movement of water, heat, and multiple solutes in variably-saturated media. *Technical manual,* Vers 1.0. PC Progress, Prague, Czech Republic.

[11] Skaggs TH, Trout TJ, Simunek J, Shouse PJ. 2004. Comparison of Hydrus-2D simulations of drip irrigation with experimental observations. *Journal of Irrigation and Drainage Engineering -ASCE.* 130(4), 304-310.

[12] Crevoisier D, Popova Z, Mailhol JC, Ruelle P. 2008. Assessment and simulation of water and nitrogen transfer under furrow irrigation. *Agricultural Water Management.* 95(4), 354-366.

[13] Kandelous MM, Simunek J. 2010. Comparison of numerical, analytical, and empirical models to estimate wetting patterns for surface and subsurface drip irrigation. *Irrigation Science.* 28, 435-444.

[14] Ravikumar V, Vijayakumar G, Simunek J, Chellamuthu S, Santhi R, Appavu K. 2011. Evaluation of fertigation scheduling for sugarcane using a vadose zone flow and transport model. *Agricultural Water Management.* 98(9), 1431-1440.

[15] Ramosa TB, Simunek J, Gonçalvesa MC, Martinsc JC, Prazeresc A, Pereiraa LS. 2012. Two-dimensional modeling of water and nitrogen fate from sweet sorghum irrigated with fresh and blended saline waters. *Agricultural Water Management.* 111, 87-104.

[16] Siyal AA, Van Genuchten MTH, Skaggs TH. 2013. Solute transport in a loamy soil under subsurface porous clay pipe irrigation. *Agricultural Water Management.* 121, 73-80.

[17] Blunt M. 2001. Flow in porous media - pore-network models and multiphase flow. *Current Opinion in Colloid & Interface Science.* 6, 197–207.

[18] Blunt M, Jackson MD, Piri M, Valvatne PH. 2002. Detailed physics, predictive capabilities and macroscopic consequences for pore-network models of multiphase flow. *Advances in Water Resources.* 25, 1069–1089.

[19] Celia MA, Reeves PC, Ferrand LA. 1995. Recent advances in pore scale models for multiphase flow in prous media. *Reviews of Geophysics.* 33 (S1), 1049–1058.

[20] Fatt I. 1956. The network model of porous media, I, Capillary pressure characteristics. *Petroleum Transaction, AIME.* 207, 144–159.

[21] Koplik J, Lasseter TJ. 1985. Two-phase flow in random network models of porous media. *Society of Petroleum Engineers Journal.* 25, 89–110.

[22] Touboul E, Lenormand R, Zarcone C. 1987. Immiscible displacements in porous media: testing network simulators by micromodel experiments, in SPE Annual Technical Conference and Exhibition, 27-30, *Society of Petroleum Engineers Journal.*

[23] Blunt M, King P, Scher H. 1992. Simulation and theory of two-phase flow in porous media. *Physical Review A.* 46, 7680–7702.

[24] Valvanides MS, Payatakes AC. 2001. True-to-mechanism model of steady-state twophase flow in porous media, using decomposition into prototype flows, *Advances in Water Resources.* 24, 385–407.

[25] Dahle HK, Celia MA. 1999. A dynamic network model for two-phase immiscible flow. *Computational Geosciences.* 3, 1–22.

[26] Singh M, Mohanty KK. 2003. Dynamic modelling of drainage through threedimensional porous materials. *Chemical Engineering Science.* 58, 1–18.

[27] Fenwick DH, Blunt MJ. 1998. Three-dimensional modeling of three phase imbibition and drainage. *Advances in Water Resources.* 21(2), 121-143.

[28] Reeves PC, Celia MA. 1996. A functional relationship between capillary pressure, saturation and interfacial area as revealed by a pore scale model. *Water Resource Research.* 32(8), 45-58.

[29] Held RJ, Celia MA. 2001. Modeling support of functional relationships between capillary pressure, saturation, interfacial area and common lines. *Advances in Water Resources.* 24, 325–343.

[30] Joekar-Niasar V, Hassanizadeh SM, Leijnse A. 2008. Insights into the relationships among capillary pressure, saturation, interfacial area and relative permeability using pore-network modeling. *Transport in Porous Media.* 74 (2), 201–219.

[31] Van Genuchten MTh. 1980. A closed-form equation for predicting the hydraulic conductivity of unsaturated soils. *Soil Science Society of American Journal.* 44, 892-898.

[32] Joekar-Niasar V, Hassanizadeh SM, Dahle HK. 2010. Non-equilibrium effects in capillarity and interfacial area in two-phase flow: dynamic pore-network modelling. *Journal of Fluid mechanics.* 655, 38–71.

[33] Richards LA. 1931. Capillary conduction of liquids in porous mediums. *Physics.* 1, 318–333.

[34] Bear J. 1988. Dynamics of Fluids in Porous Media, *Dover Publications,* New York.

[35] Besharat S, Nazemi AH, Sadraddini AA. 2010. Parametric modeling of root length density and root water uptake in unsaturated soil. *Turkish Journal of Agriculture and Forestry.* 34, 439-449.

[36] Vauclin M, Haverkamp R, Vauchaud G. 1989. Résolution de l'équation de l'infiltration de l'eau dans le sol : approches analytiques et numériques. *Presses Universitaires de Grenoble,* Grenoble, 183 pp.

[37] Shan Y, Wang Q. 2012. Simulation of salinity distribution in the overlap zone with double-point-source drip irrigation using HYDRUS-3D. *Australian Journal of Crop Science.* 6(2), 238-247.